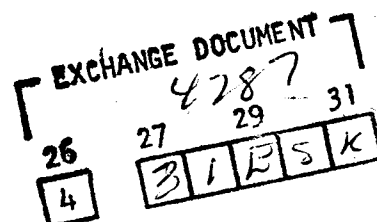
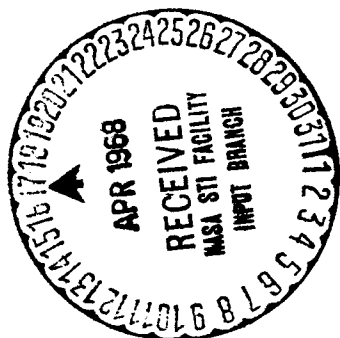


10257

SCIENTIFIC NOTE

ESRO SN-12

December 1967



GPO PRICE \$ _____

CSFTI PRICE(S) \$ _____

Hard copy (HC) 300Microfiche (MF) 65

ff 653 July 65

ESRO

Fe I, Cr I AND Cr II gf-VALUES FROM SHOCK-TUBE MEASUREMENTS

by M. Huber and F. L. Tobey, Jr.
Harvard College Observatory
Cambridge, Mass., U.S.A.

FACILITY FORM 602

N 68-20405

(ACCESSION NUMBER)

(THRU)

51

(PAGES)

(CODE)

CR-93856

(NASA CR OR TMX OR AD NUMBER)

(CATEGORY)

ORGANISATION EUROPÉENNE DE RECHERCHES SPATIALES
 EUROPEAN SPACE RESEARCH ORGANISATION

SCIENTIFIC NOTE

ESRO SN-12

December 1967

Fe I, Cr I AND Cr II gf-VALUES FROM SHOCK-TUBE MEASUREMENTS

by M. Huber and F. L. Tobey, Jr.

Harvard College Observatory

Cambridge, Mass., U.S.A.

ORGANISATION EUROPÉENNE DE RECHERCHES SPATIALES
EUROPEAN SPACE RESEARCH ORGANISATION

114, avenue de Neuilly, 92 Neuilly-sur-Seine (France)

ESRO Scientific and Technical Notes are informal documents reporting on scientific or technical work carried out by the Organisation or on its behalf. The work reported was done under an ESRO Research Fellowship and does not necessarily reflect the policy of the Organisation.

PRECEDING PAGE³ BLANK NOT FILMED.

Abstract

Measurements of f -values by the absorption technique from a shock-heated gas are described. The line emission from the hot gas has made it necessary to apply corrections to the observed equivalent widths. Considerable line widths which are due almost exclusively to Van der Waals broadening have been observed. A correction for the resulting line wing absorption has been incorporated into the data reductions.

The results show disagreements with gf -values of Corliss et al. (arc measurements) on the absolute scale and with lines which have an upper excitation potential exceeding $48\,000\text{ cm}^{-1}$ on the relative scale. The latter discrepancy is attributed to a partially erroneous normalization function used in the previous measurements on an open arc.

FE I, CR I AND CR II GF-VALUES FROM SHOCK TUBE MEASUREMENTS

I.	§ 1.	Introduction	1
II.	§ 2.	Experimental	3
III.		Results	
	§ 3.	Summary	10
	§ 4.	Determination of number densities	13
	§ 5.	Determination of equivalent width; correction for emission, line wings and non-linear curve of growth.	15
IV.	§ 6.	Conclusions	26
		Acknowledgements	40
		References	41
		Table	45

LIST OF FIGURES

Fig. 1. Experimental arrangement.

Fig. 2. Block scheme of electronics and
time sequence of experiment.

Fig. 2a. Oscilloscope record of a shock.

Fig. 3. Curve of growth (from Charatis, 1961).

Fig. 4. Line profiles.

Fig. 5. A plot of $w_{\lambda}^{\text{em}}/w_{\lambda}$ (observed values)
vs. λ .

Fig. 6. A comparison of gf-values of Corliss
and Warner (1966) with present meas-
urements plotted vs. upper energy
level E2.

Fig. 6a. A comparison of corrected gf-values
of Corliss and Warner (1966) to
present measurements plotted versus
upper energy level E2.

Fig. 7. A comparison of gf-values of Corliss and Warner (1966) with present measurements plotted vs. full Lorentzian half-width.

Fig. 7a. Plot of Fig. 7 with corrected literature values.

Fig. 8. A comparison of gf-values of Corliss and Warner (1966) with present measurements plotted vs. $\log gf$.

Fig. 8a. Plot of Fig. 8 with corrected literature values.

Fig. 9. A comparison of gf-values of Corliss and Warner (1966) with present measurements plotted vs. wavelength.

Fig. 9a. Plot of Fig. 9 with corrected literature values.

FE I, CR I AND CR II GF-VALUES
FROM SHOCK TUBE MEASUREMENTS

By

Martin Huber and Frank L. Tobey, Jr.†
Harvard College Observatory

February 1967

I. INTRODUCTION

§ 1. Corliss and Warner (1966) have recently published an extensive compilation of Fe I f-values of lines lying in the quartz ultraviolet. In this paper, we report independent measurements of 38 Fe I f-values which were obtained by a shock tube absorption technique.

The upper excitation potential of the majority of the lines reported here exceeds $48\,000\text{ cm}^{-1}$, and thus falls in

†Presently with McDonnell Aircraft Corporation, St. Louis, Missouri.

a range where the normalization function pertaining to the population of the upper levels in the arc used by Corliss and Bozman (1962) has been questioned because it leads to peculiarities in solar abundance (Warner, 1964; Pagel, 1965).[†] Since this same normalization function is still used in Corliss and Warner's new compilation (1966), a comparison with a method independent of the upper level populations is desirable.

The conventional pressure-driven shock tube, which generates a uniform sample of hot gas of well-defined extent and temperature, is an eminently suitable source for this purpose. Recent experiments (Garton, Parkinson and Reeves, 1965) yielding identical line-reversal temperatures from simultaneous measurements on normal and autoionizing lines, have established that the condition of local thermal equilibrium (LTE) is well fulfilled in the region behind the reflected shock. Furthermore, transitions to upper levels above $48\,000\text{ cm}^{-1}$ can be observed in the ultraviolet absorption spectra, since the pertinent lower levels are well populated at the typical temperatures of $5000 - 6000^\circ\text{ K}$.

[†]For a discussion of this topic, see I.A.U. Symp. No. 26 on the Abundance Determination from Stellar Spectra held at Utrecht, 1964; Proceedings edited by H. Hubenet (1966).

By introducing metal atoms in the form of volatile compounds pre-mixed in known ratios with the test gas (Charatis, 1961; Wilkerson, 1961), one can calculate in principle the number densities of the various species. Thus absolute f-values may be obtained.

II. EXPERIMENTAL

§ 2. The oscillator strengths reported here were determined by photographing the absorption spectrum of shock-heated argon containing fractional percentages of iron and chromium. The techniques for flash absorption spectroscopy behind a reflected shock wave have been described in detail by Garton, Parkinson and Reeves (1964). Briefly, a uniform slug of hot gas is produced between the front of a reflected shock and the end wall of a shock tube. The sample lasts about 300 μ s, during which time an absorption spectrogram and a temperature measurement are made.

Our experimental arrangement consisted of a gas-handling system, a shock tube, a small xenon flash tube and a monochromator for line-reversal temperature measurements, as well as a flashed continuum light source and spectrograph equipped with a fast shutter for photographing the absorption spectrum. The

optical axes were perpendicular to each other and to the axis of the shock tube, intersecting the latter immediately ahead of the end wall. A schematic diagram of the experiment is shown in Fig. 1.

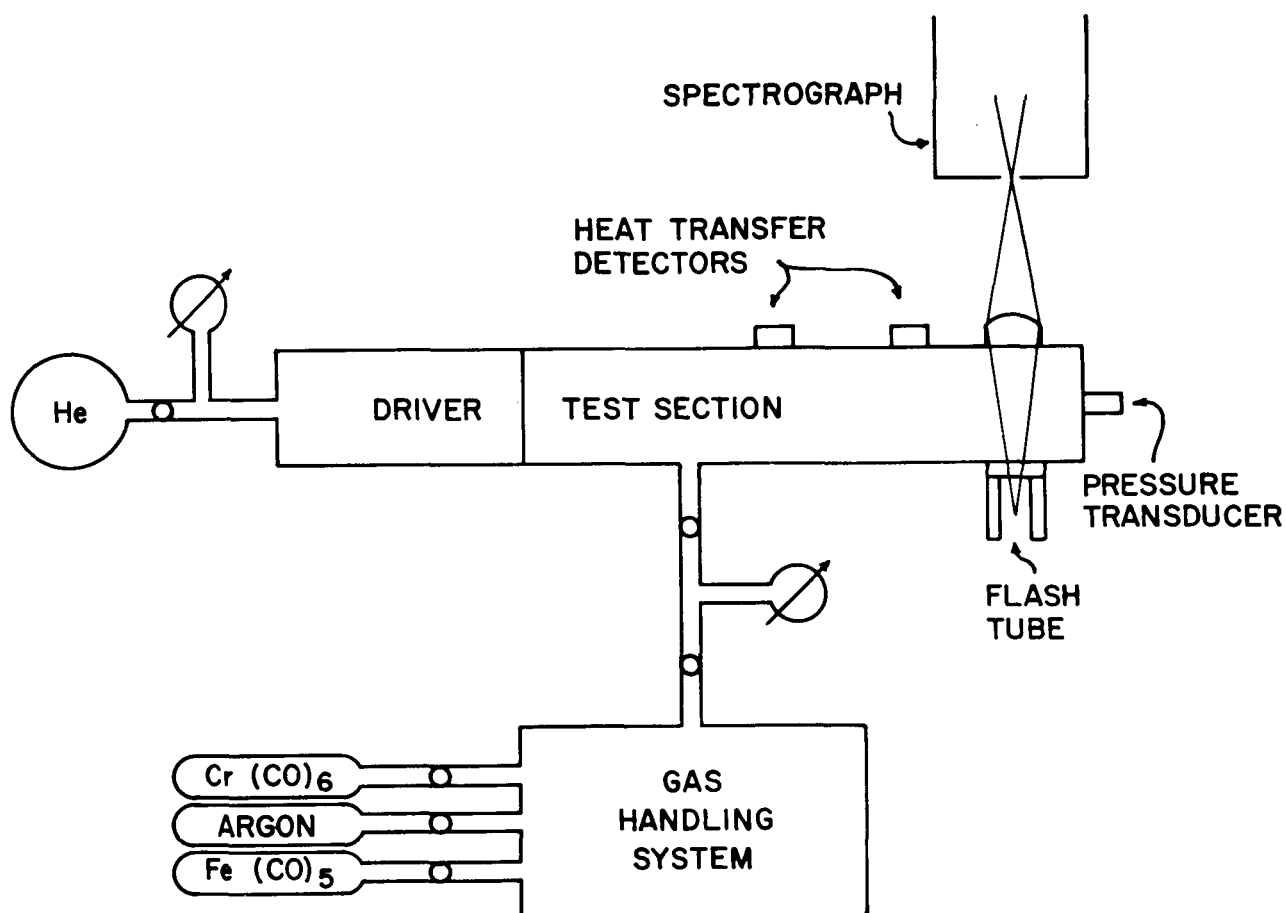


Figure 1.- Experimental arrangement; (the optical system for temperature measurements is omitted).

The gas-handling system was equipped with a Baratron capacitive sensor gauge allowing continuous pressure readings in the

range of 10^{-3} to 10 Torr, and with an absolute mechanical gauge for measuring higher pressures. The magnetically stirred storage vessels were covered to minimize possible photo-decomposition of the compounds they contained. The whole system was designed so that the mixed gases contacted only Pyrex, stainless steel, Teflon and Viton A during preparation and storage.

The stainless steel shock tube had a two-inch square internal cross section and was divided into four- and twelve-foot driver and test sections respectively. Scribed aluminum diaphragms which separated the sections were burst by over-pressure of the driver gas.

Initial test gas pressures in the shock tube were at or near 30 Torr in all cases. The driver gas was helium at pressures of 400 to 500 psi. These initial conditions resulted in incident-shock Mach numbers of about 5. Consequently the temperatures and pressures behind the reflected shock ranged from 5500 to 6000° K, and 6 to 7 atm respectively. The resulting total number densities were of the order of $8 \times 10^{18} \text{ cm}^{-3}$.

The brightness-emissivity method as described by Parkinson and Reeves (1964) was used for measuring the temperature of the gas behind the reflected shock. The center of the shock tube was focussed onto the slit of an f/12 (effective) monochromator equipped with a 600 ℓ/mm concave grating in a Johnson-Onaka

mounting (Johnson, 1957; Onaka, 1958), giving a reciprocal dispersion of 32 \AA/mm . A photomultiplier mounted at the exit slit monitored the emission of the shocked gas at the 3859.91 \AA Fe I line. The shock absorptivity (or emissivity) at this wavelength was sampled with a 5 \mu s flash from a continuum light source (FX-12 xenon flash lamp) focussed into the center of the shock tube and refocussed onto the monochromator slit. A calibrating flash in the absence of the shock and a comparison of the shock brightness with the emission from a standard lamp provided the information necessary for the line-reversal temperature determination.

A large aperture coaxial flash tube of the type used by Garton (Wheaton, 1964) provided the background continuum for the absorption spectra. A plano-convex quartz lens mounted in the shock tube wall focussed the flash tube radiation onto the slit of the spectrograph. This was a 3-meter Eagle-mounted concave grating instrument (McPherson Instrument Company) with an effective speed of $f/26$ and an inverse dispersion of 2.78 \AA/mm . A 100 \mu m wide slit was used. Thus the spectrograph operated as an integrating device, the line profiles showed flat bottoms and the resulting line depth was a measure of the total line absorption. The wide slit also permitted the use of medium slow Kodak Spectrum Analysis Number 1 plates, which have high con-

trast and a very fine grain.

Calibration continua were placed on all plates by photographing the background source through a series of calibrated neutral density filters. The developed plates were traced with a Joyce-Loebl dual-beam microdensitometer employing a scanning spectral slit width of 28 mÅ.

Fig. 2 shows a schematic diagram of the electronics and the time sequence of the experiment. The velocity of the incident shock is obtained from the time delay between two pulses

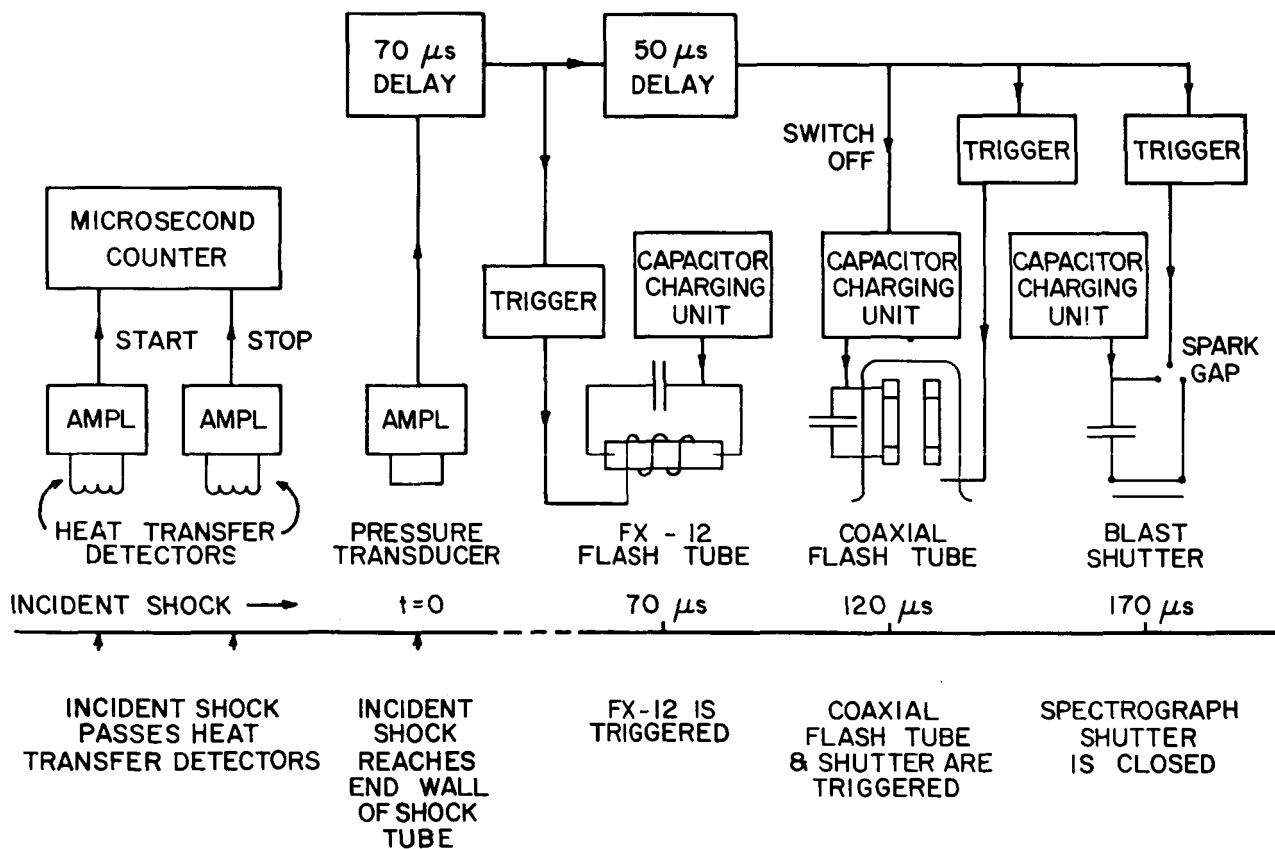


Figure 2.- Block scheme of electronics and time sequence of experiment.

originating from two heat transfer detectors of a known separation. The reflection of the shock at the end wall actuates a pressure transducer and thus defines time "zero" for the electronics. The delay units trigger a) the FX-12 flash tube 70 μ s later and b) the coaxial flash tube and the spectrograph shutter after an additional 50 μ s.

Fig. 2a is a reproduction of an actual record of the emission from a reflected shock as it was observed at the exit slit of the monochromator as well as near the focal plane of the spectrograph. The record indicates that a minimum time delay of 50 μ s after reflection at the end wall was required to ensure that equilibrium was established at the shock tube windows.

It was also necessary to use a spectrograph shutter in order to reduce the long duration emission from the shocked gas, which would otherwise "fill in" the absorption spectrum. The shutter was patterned after one described by Wurster (1957), where a shock wave originating from an exploding wire is used to drive an expendable shutter (black Scotch electrical tape applied to a strip of .005-inch thick Teflon sheet) across the light beam. Closure time after firing was approximately 50 μ s. Nevertheless, the shutter did not reduce the line emission reaching the plate to a negligible level. A correction, therefore, had to be determined by the following experiment. The

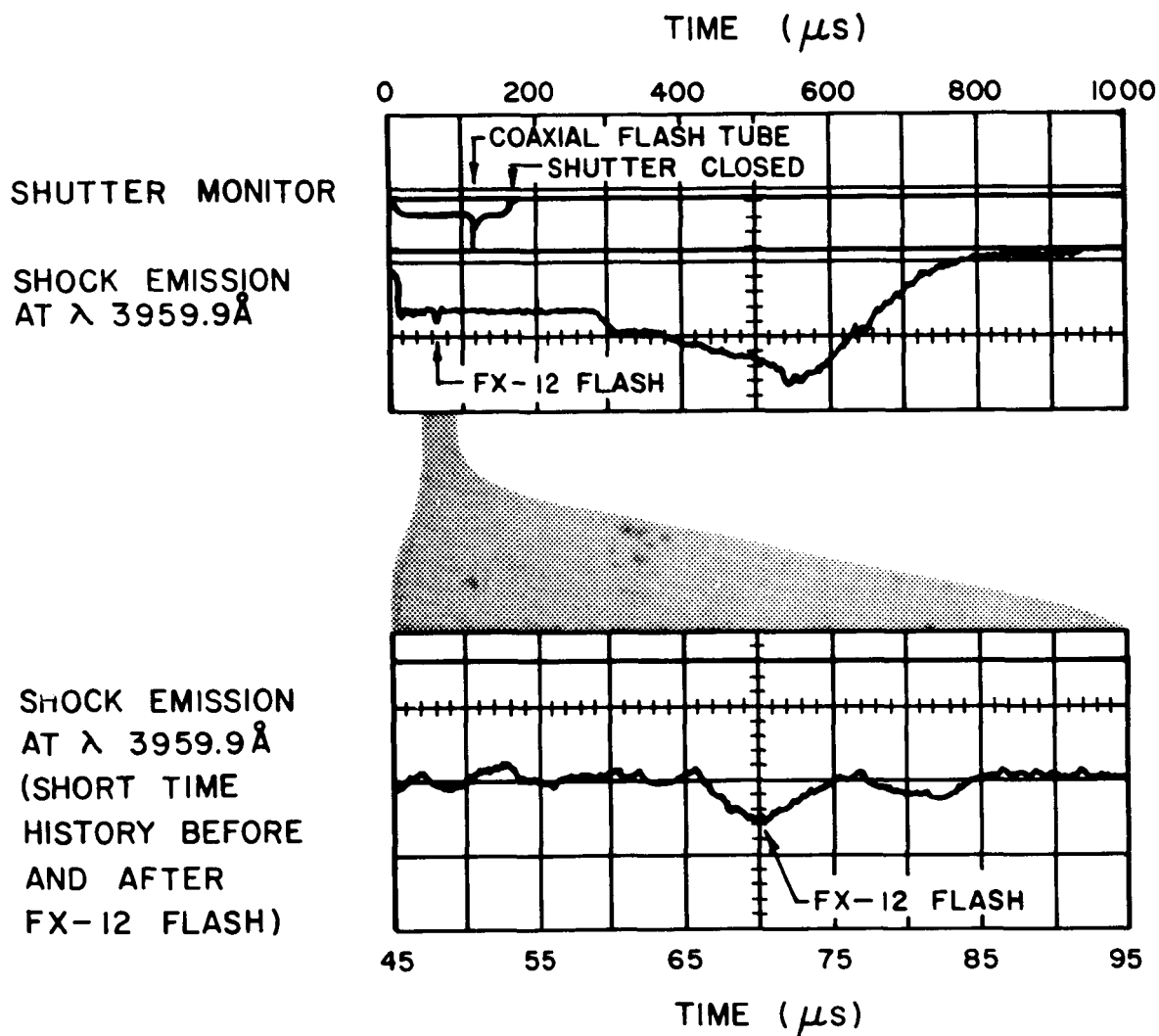


Figure 2a.- Oscilloscope record of a shock. The three traces show photo-multiplier outputs (negative voltages): Upper: Shutter monitor, 100 μs/cm. Middle: Shock emission at λ 3959.9 Å, long time history, 100 μs/cm. Lower: Short time history of signal in middle trace: $t = 45 \mu s$ to $t = 95 \mu s$.

background source was fired before initiating the shock so that the line emission was photographed on top of the continuum exposure. This line emission, measured relative to the continuum, then gave an "effective emission equivalent width" (see § 5),

which was applied to the equivalent widths measured on the absorption plates.

Three different concentrations of iron and chromium carbonyls in argon were used in the experiments: 0.05 per cent Cr, 0.2 per cent Fe; 0.02 per cent Cr, 0.15 per cent Fe; and 0.0015 per cent Cr, 0.2 per cent Fe. The carbonyl pressures used in preparing the mixtures were kept below about half their vapor pressures at room temperature to preclude errors due to saturation. Data were taken on a total of 18 shocks distributed among the three concentrations. In addition an emission spectrogram on plates pre-exposed to the continuum light source as described above was photographed for each of the three mixtures.

A spectrum was also obtained with a narrow (10 μ m) slit, using a fast emulsion (Kodak Spectroscopic Plate I-0) at a concentration of .01 per cent Cr and .3 per cent Fe. Density scans provided line width data which were used for the wing correction (see § 5).

III. RESULTS

§ 3. Summary. The data reduction is based on a "curve of growth" (Fig. 3) relating the line equivalent width, W_{λ} ,

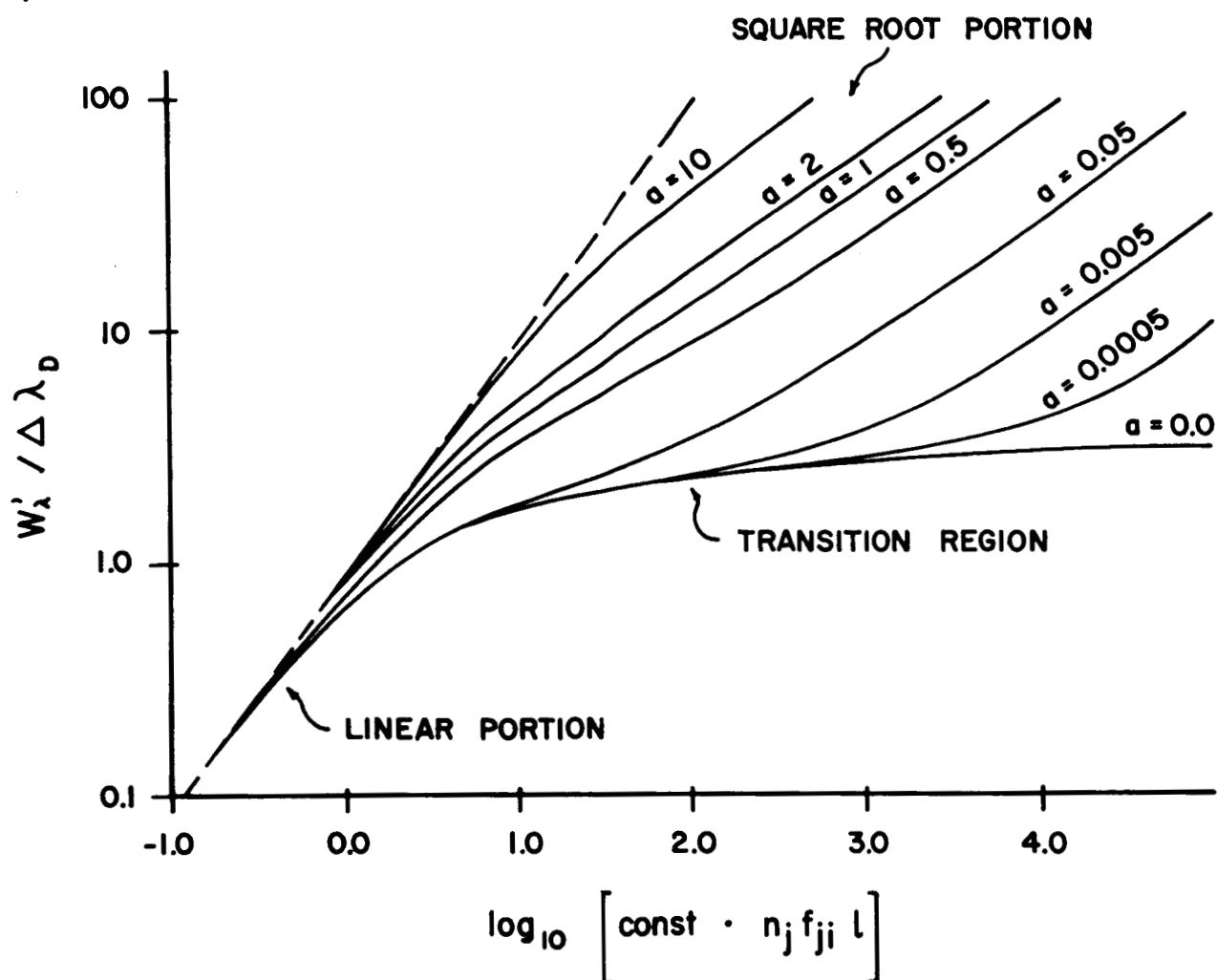


Figure 3.- Curve of growth (from Charatis, 1961).

to the product $n^* \cdot f \cdot l$, where n^* is the population density of the absorbing state, f is the oscillator strength of the transition in question, and l is the path length in the absorbing gas layer. The relationship is linear for optically thin lines ($\frac{W_{\lambda}}{\Delta \lambda_D} \ll 1$):

$$W_{\lambda} \sim n^* \cdot f \cdot \ell$$

where $\Delta\lambda_D$ is the full $\frac{1}{e}$ -width of the Doppler component of the line profile.

For larger equivalent widths the curve of growth departs from linearity in a manner dependent on a parameter

$$a = \frac{\Delta\lambda_L}{\Delta\lambda_D}$$

where $\Delta\lambda_L$ is the full half-width of the Lorentzian component of an observed Voigt profile. Thus a determination of f requires knowledge of W_{λ} , of n^* along the path length ℓ , and of a , if the lines are not optically thin.

For the conditions of this experiment the boundary layer was negligible so that (as implied in the above notation) n^* was uniform and ℓ equal to the separation of the shock-tube windows. The n^* were computed from the total number densities n_i of the pertaining ion species by the Boltzmann equation. The n_i in turn were determined by solving the Saha equation for the gases existing behind the reflected shock.

The equivalent widths obtained from the densitometer traces of the plates were corrected for shock emission as well

as for absorption of the line wings lying beyond the limits of the slit width used and thus not integrated by the spectrograph. Both these corrections increased the equivalent widths actually measured on the plates.

The lines used were selected with the criterion that no line of detectable intensity should lie closer than $280 \text{ m}\text{\AA}$ (the spectral slit width) to the line under investigation. This was done with the aid of the second revision of Rowland's Preliminary Table of Solar Spectrum Wavelength (Moore et al., 1966). This catalogue is the most recent collection of lines and also provides quantitative data expressed as reduced solar equivalent widths. Because the Fraunhofer lines of interest to this work are formed by the absorption of gases at temperatures similar to those obtained in the shock tube, the solar equivalent widths were a useful indicator of the relative line intensities to be expected in our experiments.

Most of the lines were unblended. In a few cases where two lines fell at the same wavelength ($\Delta\lambda < 280 \text{ m}\text{\AA}$), the sum of the f-values is reported. Oscillator strengths were obtained for 45 lines in all, 38 of Fe I, 5 of Cr I and 2 of Cr II. The results are listed in table 1.

§ 4. Determination of number densities. The number densities of the components of a gas consisting of several atomic, molecular

and ion species in local thermodynamic equilibrium, is given by the solutions of a system of simultaneous equations including the equilibrium relations for dissociation and ionization (Saha equations), and the conservation of charge and mass equations. The coefficients in these equations are the partition functions, elemental concentration, temperature and total pressure. The total pressure P_5 behind the reflected shock was computed from the hydrodynamic expressions:

$$P_5 = \left\{ \frac{2\gamma M^2 - (\gamma - 1)}{\gamma + 1} \right\} \left\{ \frac{(3\gamma - 1)M^2 - 2(\gamma - 1)}{(\gamma - 1)M^2 + 2} \right\} P_1 \quad (1)$$

where γ is the ratio of specific heats ($\gamma = \frac{c_p}{c_v}$) taken to be 5/3. P_1 , the initial pressure of the test gas is read from a mechanical gauge and M , the incident-shock Mach number is calculated from the measured shock velocity and the sound velocity in Argon at 298° K (0.321 mm/ μ s).

The increase in P_5 which was due to the CO, C₂, O₂, C and O molecules and atoms originating from the dissociated carbonyls amounted to only 2.7 per cent of the total in the most extreme case. This and other real-gas effects which are not taken into account in eq. (1) are known to be small (cf. e.g. Gaydon and Hurle, 1963) and therefore were neglected.

The Saha equations covered the following species and their first ionization stages: A, C, Cr, Fe, O, C₂, CO, CrO, FeO, O₂ and CO₂. Atomic partition functions required for the Saha and Boltzmann relations were interpolated between values taken from the tables of Drawin and Felenbok (1965). Partition functions for the molecules were computed from their molecular constants.

The solutions to the Saha equations were obtained on an IBM 7094 computer using the EXCIT 4 program of Rich and Flagg (1966).

§ 5. Determination of equivalent width; correction for emission, line wings and non-linear curve of growth. With the 100 μm wide spectrograph slit, each point on the plate records radiation from a spectral bandwidth of 280 mÅ. The intensity received at a location x on the plate (cf. Fig. 4) is described by two terms representing absorption and emission respectively:

$$I_x = \int_{\Delta t_F} \int_{\lambda_x - \frac{\Delta\lambda_o}{2}}^{\lambda_x + \frac{\Delta\lambda_o}{2}} S(\lambda) B_\lambda(T_F(t)) \cdot e^{-\tau_\lambda(t)} d\lambda dt + \int_{\Delta t_S} \int_{\lambda_x - \frac{\Delta\lambda_o}{2}}^{\lambda_x + \frac{\Delta\lambda_o}{2}} S(\lambda) B_\lambda(T_S(t)) (1 - e^{-\tau_\lambda(t)}) d\lambda dt \quad (2)$$

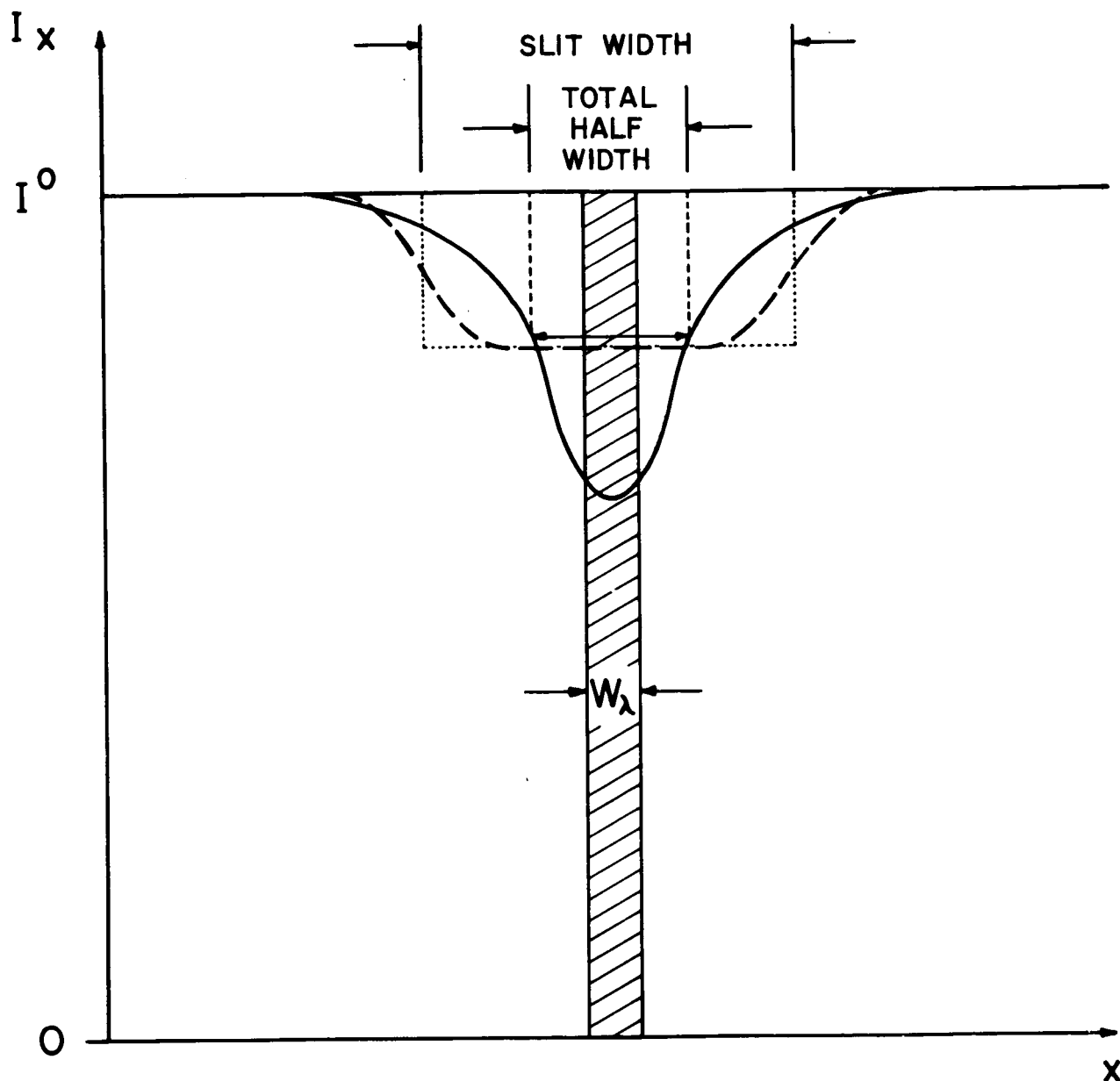



Figure 4.- Line profiles.

- true profile (x represents λ)
- - - profile recorded on plate
- rectangular equivalent for area under recorded profile
-  rectangular profile defining equivalent width

where

$S(\lambda)$ = slit function

$\tau_{\lambda}(t)$ = optical depth of shocked gas at wavelength λ

$T_F(t)$ = brightness temperature of the coaxial flash tube

$T_S(t)$ = thermodynamic shock temperature

$B_{\lambda}(T)$ = black body function

λ_x = wavelength recorded at x , assuming an infinitely narrow slit (cf. Fig. 4)

$\Delta\lambda_0$ = spectral slit width (278 mÅ)

Δt_F = duration of flash tube emission ($\approx 3 \mu s$)

Δt_S = duration of shock tube emission ($\approx 170 \mu s$)

The following assumptions are made in the present experiment:

- that the slit function is rectangular
- that B_{λ} can be replaced by a constant B_{λ_x} (within the spectral slit width $\Delta\lambda_0$)
- that $\tau_{\lambda}(t)$ does not vary during the flash duration Δt_F (this last assumption implies that heating of the shock by the flash tube is negligible).

Eq. (2) is then simplified to

$$I_x = \int_{\lambda_x - \frac{\Delta\lambda_o}{2}}^{\lambda_x + \frac{\Delta\lambda_o}{2}} e^{-\tau_\lambda} d\lambda \cdot \int_{\Delta t_F} B_{\lambda_x} (T_F(t)) dt + \int_{\Delta t_S} B_{\lambda_x} (T_S(t)) \int_{\lambda_x - \frac{\Delta\lambda_o}{2}}^{\lambda_x + \frac{\Delta\lambda_o}{2}} (1 - e^{-\tau_\lambda(t)}) d\lambda dt \quad (3)$$

and the continuum intensity is obtained by setting $\tau_\lambda(t) = 0$:

$$I^o = \Delta\lambda_o \int_{\Delta t_F} B_{\lambda_x} (T_F(t)) dt . \quad (4)$$

It also follows that the equivalent width w_λ which is defined by

$$w_\lambda = \int_{\text{line}} (1 - e^{-\tau_\lambda}) d\lambda \quad (5)$$

can be expressed by the simple formula

$$w_\lambda = \frac{I^o - I_x}{I^o} \Delta\lambda_o .$$

as long as line radiation may be neglected and if the spectral slit width covers the whole line profile.

However, in this experiment the line emission may not be overlooked. Although the black-body function of the flash tube

$B_{\lambda_x}(T_F)$ is much larger than that of the shock tube $B_{\lambda_x}(T_s)$ (with T_F and T_s of the order of 28 000°K and 5500°K respectively), the much longer duration of the shock radiation ($\Delta t_s \approx 170\mu s$ vs. $\Delta t_F \approx 3\mu s$) tends to balance the energy absorbed from the continuum. The size of the correction due to emission was determined from the experiments in which the flash tube was fired previous to the initiation of the shock, so that the emission lines from the shocked gas appeared superimposed on the background continuum. By adapting equations (3), (4), and (5) for this case, one obtains I_x^{em} , the integrated intensity at the location of an emission line:

$$I_x^{em} = I^{\circ} + \int_{\Delta t_s} B_{\lambda_x}(T_s(t)) W_{\lambda}(t) dt \quad (6)$$

The true absorption intensity is then

$$I_x^{abs} = I_x - (I_x^{em} - I^{\circ}) \quad (7)$$

where I_x is the intensity initially measured on our absorption spectra at the position of a line. The corrected equivalent width can be written as

$$W_{\lambda}^{abs} = \frac{I^{\circ} - I_x^{abs}}{I^{\circ}} \Delta\lambda_0 = \frac{I^{\circ} - [I_x - (I_x^{em} - I^{\circ})]}{I^{\circ}} \Delta\lambda_0 = W_{\lambda} + W_{\lambda}^{em} \quad (8)$$

where we define an "effective emission equivalent width" by

$$w_{\lambda}^{\text{em}} = \frac{I_x^{\text{em}} - I^{\circ}}{I^{\circ}} \Delta\lambda_0 .$$

For the preceding formula we have assumed identical shock and flash tube behavior for different trials; while this is not strictly true, the random error introduced into w_{λ}^{em} by the photometry exceeds the effects of variations between shocks on the correction for emission.

Fig. 5 shows a plot of $\frac{w_{\lambda}^{\text{em}}}{w_{\lambda}}$ vs. wavelength for a series of six shocks, one in emission and one in absorption for each of the three concentrations of Fe and Cr used. While there is considerable scatter, averaging the values at or near the same wavelength yielded a set of points which could be approximated by a straight line curve. We note that the correction increases with wavelength. Qualitatively, this is the behavior expected since the emission from a 5500° K black body increases with wavelength in this region, while the emission from a 25 000°K black body decreases with wavelength. The correction for emission thus was made with the aid of the plot in Fig. 5, viz.,

$$w_{\lambda}^{\text{abs}} = w_{\lambda} \left(1 + \frac{w_{\lambda}^{\text{em}}}{w_{\lambda}} \right)$$

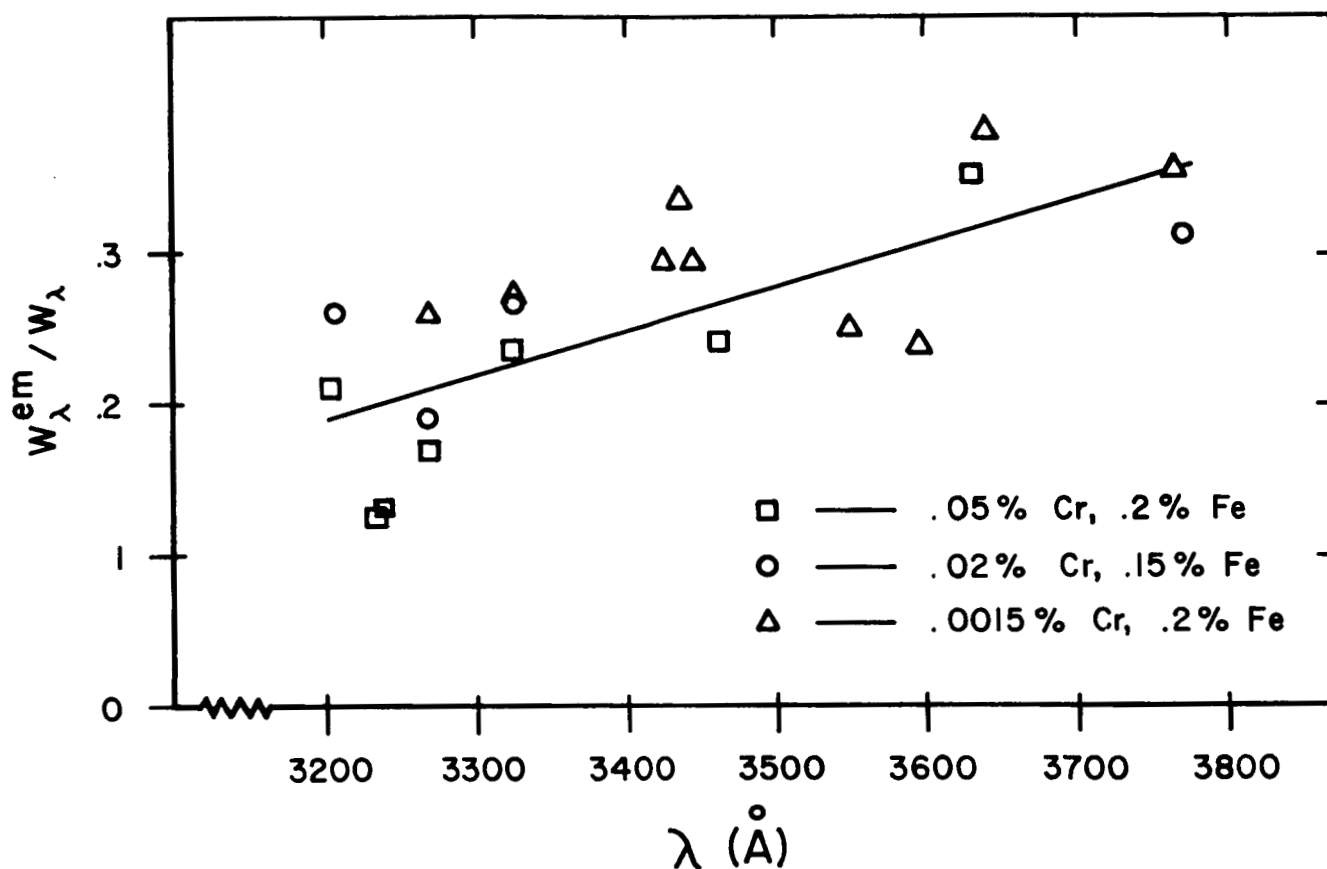


Figure 5.- A plot of $W_{\lambda}^{\text{em}} / W_{\lambda}$ (observed values) vs. λ . Results are taken from six shocks, one in emission and one in absorption for the three concentrations used.

The second assumption made above, i.e. that the spectral slit width includes the whole absorption profile of a line, means that the integration limits $\lambda_x \pm \frac{\Delta\lambda_0}{2}$ in equation (3) can be set formally to infinity without changing the value of the integral. This condition is extremely hard to fulfill if Lorentzian broadening is predominant. In the case of a pure Lorentzian

line profile in absorption, the absorption lying outside the range of the slit width will still amount to 9 per cent even when $\Delta\lambda_o = 10\Delta\lambda_L$ ($\Delta\lambda_L$ = full halfwidth of line profile). The ratio $w'_\lambda/w_\lambda^{abs}$ of the actual equivalent width to measured equivalent width (which has been corrected for possible shock emission effects of the kind described above) can be written as:

$$\frac{w'_\lambda}{w_\lambda^{abs}} = \frac{\int_{-\infty}^{+\infty} \frac{dx}{1+x^2}}{\int_{\frac{-\Delta\lambda_o}{\Delta\lambda_L}}^{\frac{+\Delta\lambda_o}{\Delta\lambda_L}} \frac{dx}{1+x^2}} = \frac{\pi}{2[\text{arc tg } \frac{\Delta\lambda_o}{\Delta\lambda_L}]} \quad (11)$$

Wiese (1963) gives a detailed derivation of eq. (11) for the corresponding case of emission.

The parts of the profile relevant to this correction, viz., the cut off wings are in fact of Lorentzian type (as was assumed in eq. (11)). The full Doppler half-width in the shock-heated gas is of the order of about 30 mÅ. This corresponds to a third to a tenth of the Lorentzian half-width, as will be seen below (p. 24). Doppler broadening thus does not contribute significantly to the wing absorption.

Due to the crowding of the Fe spectral lines in the wavelength region investigated, it was not possible to widen the slit to ten Lorentzian half-widths or more without causing serious blends. A correction, therefore, was mandatory for each individual line. In order to do this, the widths of all the lines reported in Table 1 were measured from a plate taken with a narrow spectrograph slit. The half-width of the line profiles observed on the plate taken with a narrow spectrograph slit was obtained from a microdensitometer scan of the photographic density, i.e., on a density vs. wavelength plot. There, the width of absorption lines can be read off directly at the level of half the peak absorption density, provided that both the densities for continuum and peak absorption lie within the straight portion of the characteristic curve of the emulsion.

The full half-width $\Delta\lambda_V$ obtained in this way is assumed to be generated by Lorentzian and Doppler line broadening plus instrumental broadening. For simplicity, the latter was taken to be Gaussian. The instrumental slit width $\Delta\lambda_s = 0.81 \cdot \Delta\lambda_o$ (Allen, 1964) thus was combined with the full Doppler $1/e$ - width which was computed by

$$\Delta\lambda_D = \frac{2\lambda}{c} \sqrt{\frac{2kT}{m_a}} \quad (12)$$

($\approx 30 \text{ m}\text{\AA}$ in this experiment; m_a = atomic weight) to obtain the full Gaussian width

$$\Delta\lambda_G = \sqrt{\Delta\lambda_D^2 + \Delta\lambda_S^2} \quad (13)$$

The observed line profile accordingly can be assumed to be of the Voigt type, and the quantity needed for the line width correction, eq. (11), the Lorentzian width, can be determined by using the table of Davies and Vaughan (1963). These authors relate the Gaussian and Lorentzian fractions

$$F = \frac{\Delta\lambda_G}{\Delta\lambda_V} \sqrt{\ln 2} \quad \text{and} \quad L = \frac{\Delta\lambda_L}{\Delta\lambda_V}$$

for the whole range of Voigt profiles from pure Lorentzian to pure Gaussian profiles. The observed Voigt width $\Delta\lambda_V$ and the Gaussian width $\Delta\lambda_G$ computed by eqs. (12) and (13) yield F ; from the corresponding L and from $\Delta\lambda_V$ the Lorentzian width is obtained.

The values of $\Delta\lambda_0/\Delta\lambda_L$ which enter into eq. (11) range between 0.8 and 3.1. This corresponds to full Lorentzian half-widths ranging between 350 and 100 m \AA . These results are in good agreement with theoretical estimates of $\Delta\lambda_L \approx 220 \text{ m}\text{\AA}$ due to Van der Waals broadening. Resonance and Stark

broadening effects are smaller by two orders of magnitude; this is plausible since the densities of Fe and Cr atoms and of the electrons which are responsible for resonance and Stark broadening are very low compared to the total number density which is responsible for Van der Waals broadening.

The curve of growth parameter $a = \Delta\lambda_L / \Delta\lambda_D$ was also evaluated from the line half-widths observed on the plate taken with a narrow slit. The parameter a was found to be larger than 3 for all lines observed. At these large values of a , there is no inflection of the curve of growth in the transition region between the first power (i.e., linear) and half-power portion (Fig. 3). Consequently, the correction for deviation from linearity was small and insensitive to a .

Using the corrected equivalent width w_λ' , preliminary f -values were computed with the linear approximation of the curve of growth. The parameter $a = \Delta\lambda_L / \Delta\lambda_D$ then was determined for each line and the appropriate correction was read from a plot of the curve of growth (Charatis, 1961). The corrections ranged from 3 to 13 per cent.

IV. CONCLUSIONS

§ 6. Figs. 6 through 9 show comparisons of our results with previous investigations. In Fig. 6 we have plotted the difference $\log gf$ (literature) minus $\log gf$ (this experiment) vs. upper excitation energy of the respective lines. The same difference was also plotted vs. the Lorentzian line width in the shock-heated gas (Fig. 7), vs. $\log gf$ (Fig. 8), and vs. wavelength (Fig. 9).

The data points of Fig. 6 fit a curve with a flat part that extends up to $48\,000\text{ cm}^{-1}$ and bends downward above that energy. This curve quantitatively reflects the shape of the normalization function which was used by Corliss and Bozman (1962) for the number density of the emitting levels in their arc and which was also assumed in the more recent compilation of Corliss and Warner (1966). This finding established the previously suspected fact (Pagel, 1965; Warner, 1964) that the normalization function of Corliss and Bozman (1962) should be flat up to $60\,000\text{ cm}^{-1}$. We therefore made a corresponding correction of the literature values of Corliss and Warner (1966). The resulting differences between the corrected literature values and our data are plotted in Fig. 6a.

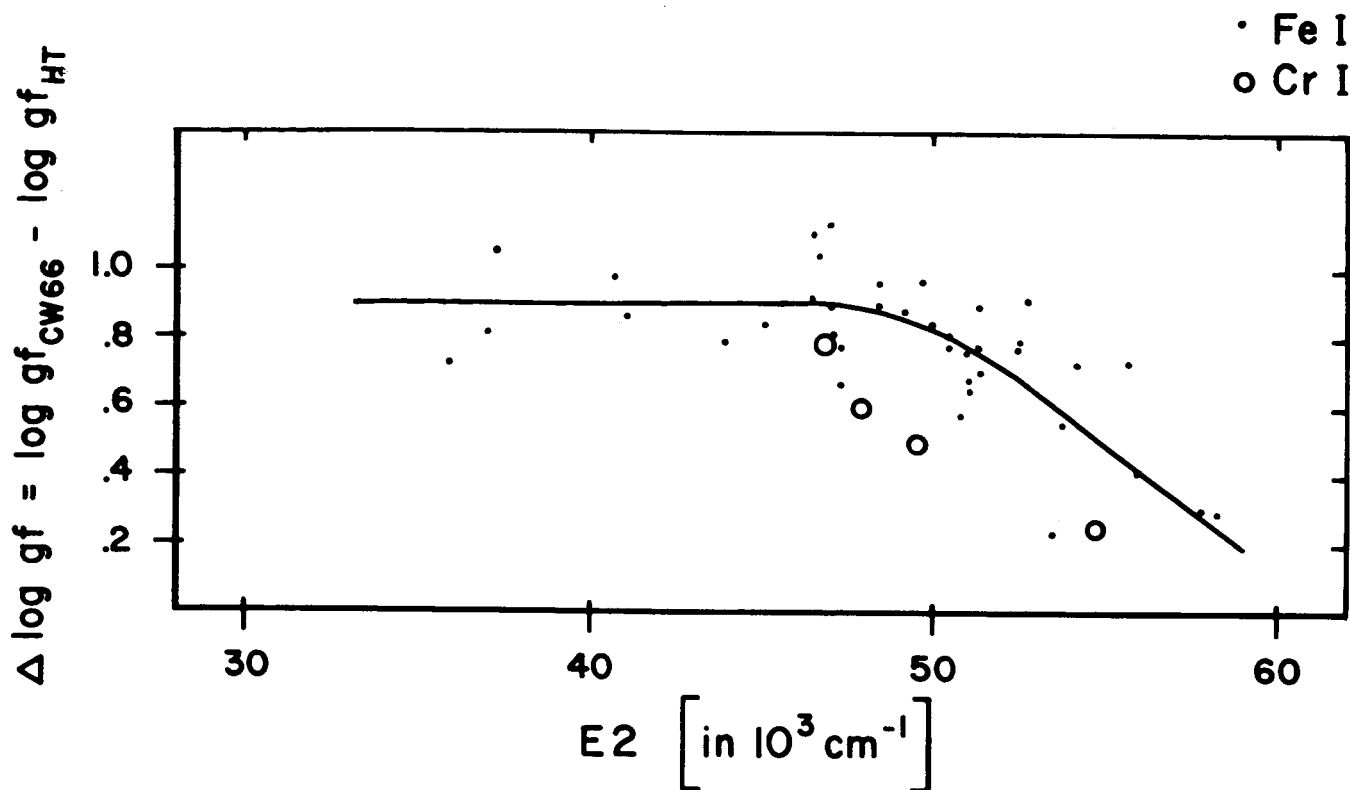


Figure 6.- A comparison of gf-values of Corliss and Warner (1966) with present measurements plotted vs. upper energy level E_2 .

— normalization function used by Corliss and Bozman (1962).

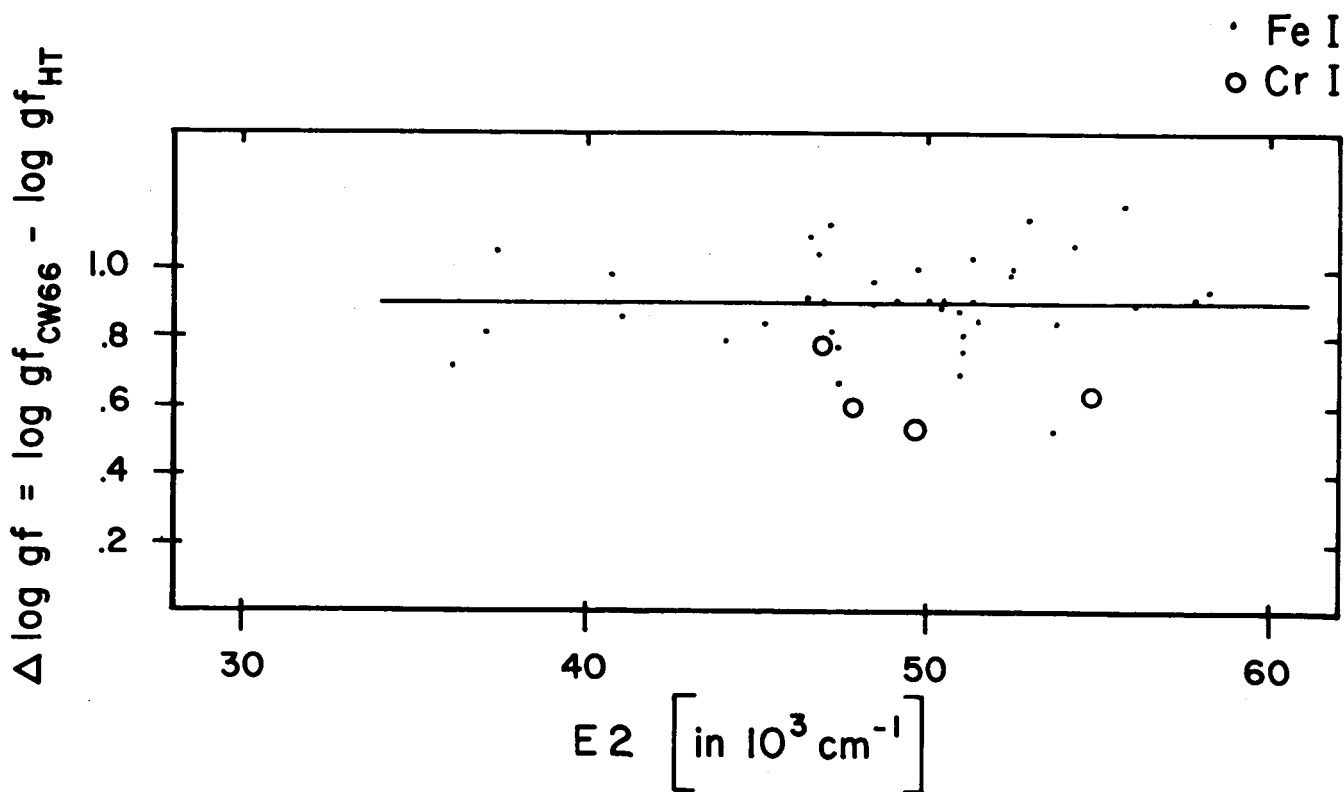


Figure 6a.- A comparison of corrected gf-values of Corliss and Warner (1966) to present measurements plotted versus upper energy level E_2 .

— corrected normalization function.

In Fig. 7, where the difference ($\log gf_{lit} - \log gf_{meas}$) is plotted vs. the (full) Lorentzian half-width of the lines observed in the shock tube spectra, there appear to be smaller differences at larger widths. This tendency disappears in Fig. 7a, where the corrected literature gf-values have been used. There is a direct correlation between the amount of Van der Waals broadening and the upper excitation energy. Therefore broad lines are more likely to be affected by the correction of the normalization function.

A trend similar to the one in Fig. 7 is apparent in Fig. 8, i.e. $\Delta \log gf$ decreases as $\log gf$ increases. Again, this behavior disappears in Fig. 8a where the corrected literature gf-values are used. The trend in Fig. 8 is due to our selection of the lines. Since a limited range of concentrations and temperatures was used in this experiment, only lines which had equivalent widths in a relatively narrow range were suitable for gf-value measurement. Consequently, since

$$W \sim gf \cdot \frac{n^*}{g} \sim \exp\left(-\frac{E}{kT}\right)$$

is approximately constant, lines with a low excitation energy E and a relatively large number density $\frac{n^*}{g}$ will have a smaller gf-value than lines with a high excitation energy and corres-

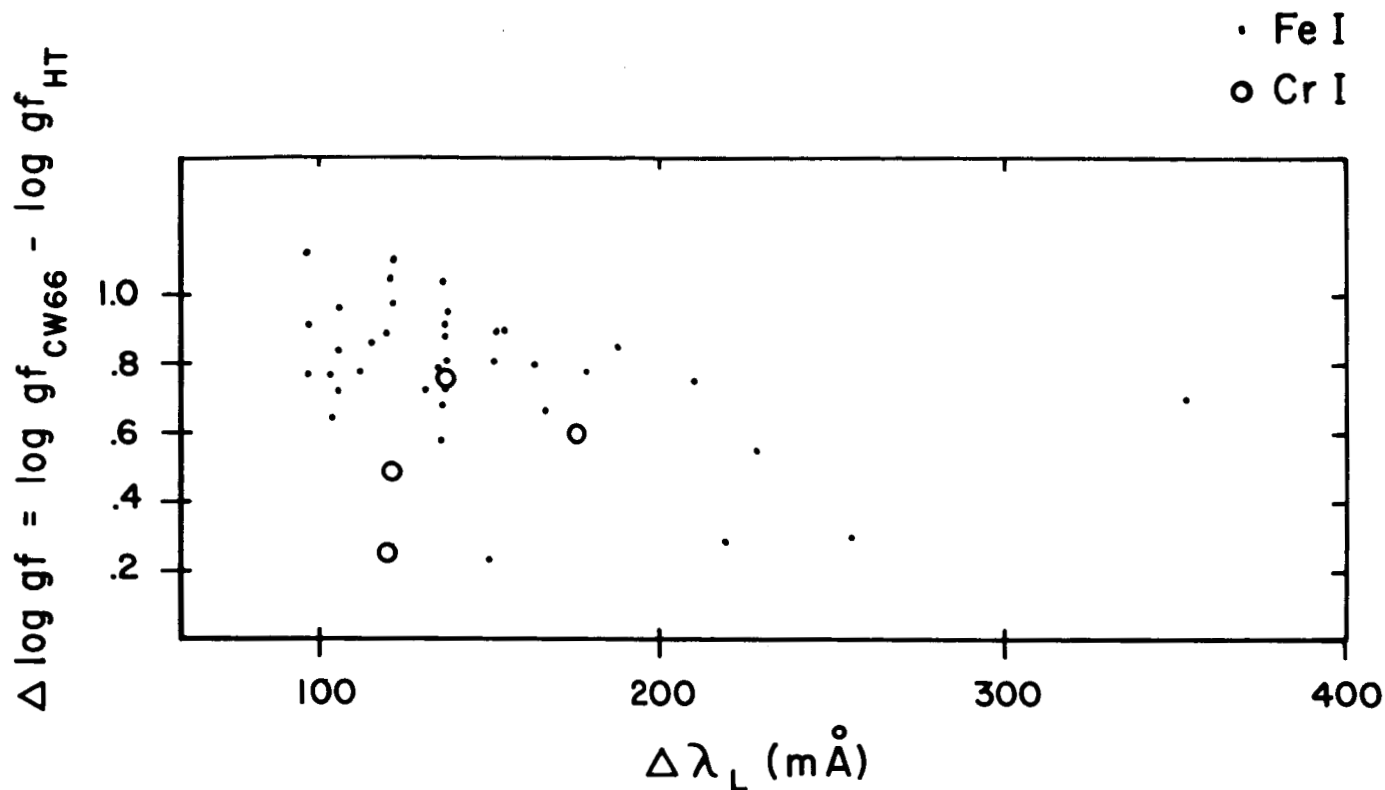


Figure 7.- A comparison of gf-values of Corliss and Warner (1966) with present measurements plotted vs. full Lorentzian half-width.

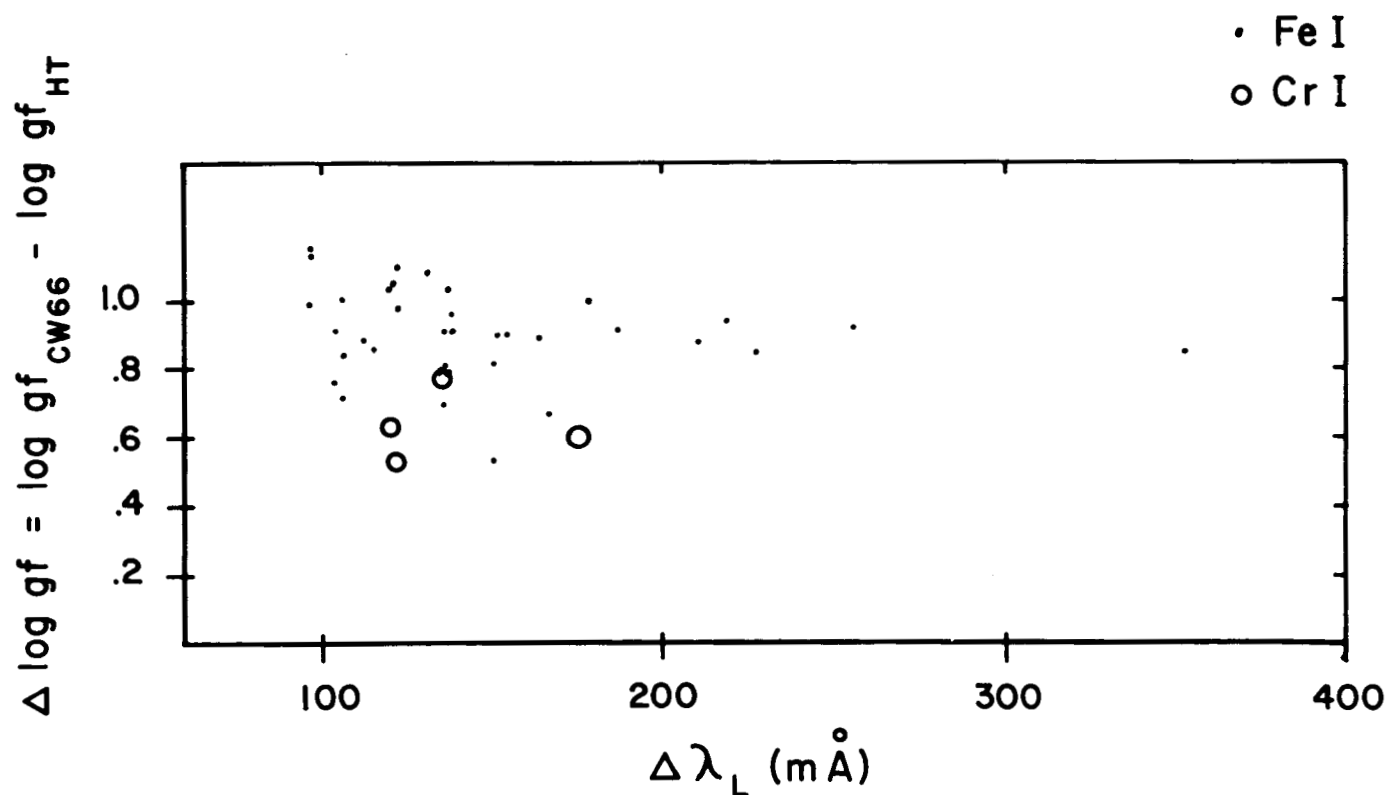


Figure 7a.- Plot of Figure 7 with corrected literature values.

ponding small number density. Furthermore, the wavelength range covered (3150-3780 Å) is limited enough so that one may interchange the lower excitation potential E1 (which should be used in the above explanation) with the upper excitation potential E2, which determines the correction of the normalization function of Corliss and Bozman (1962). The fact that the values of log gf are connected to E2 explains the apparent trend in Fig. 8.

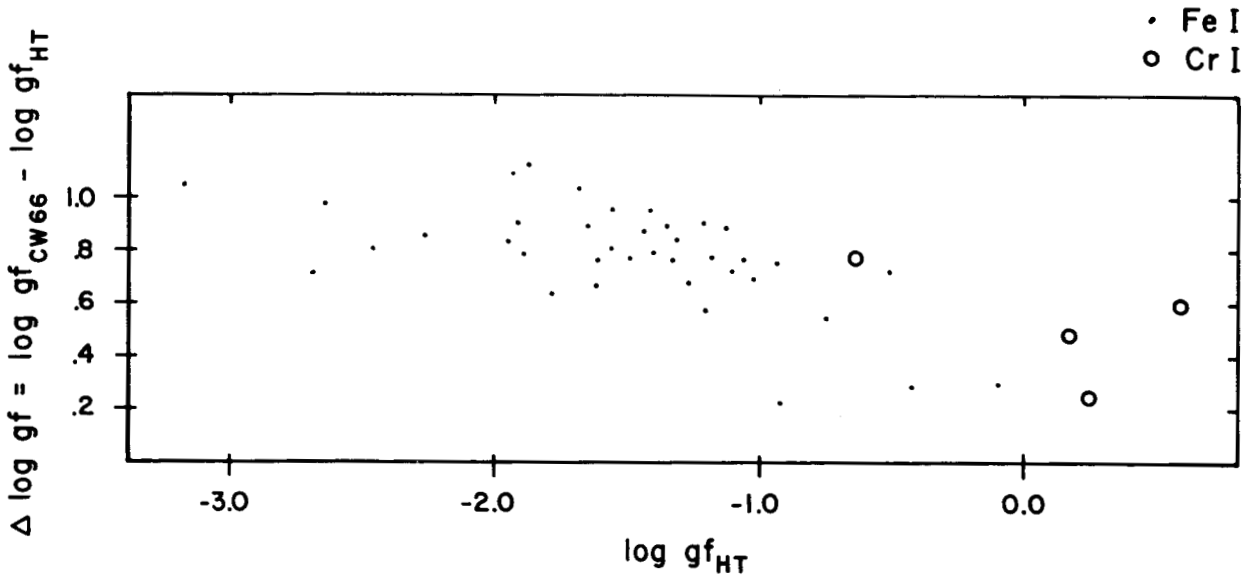


Figure 8.- A comparison of gf-values of Corliss and Warner (1966) with present measurements plotted vs. log gf.

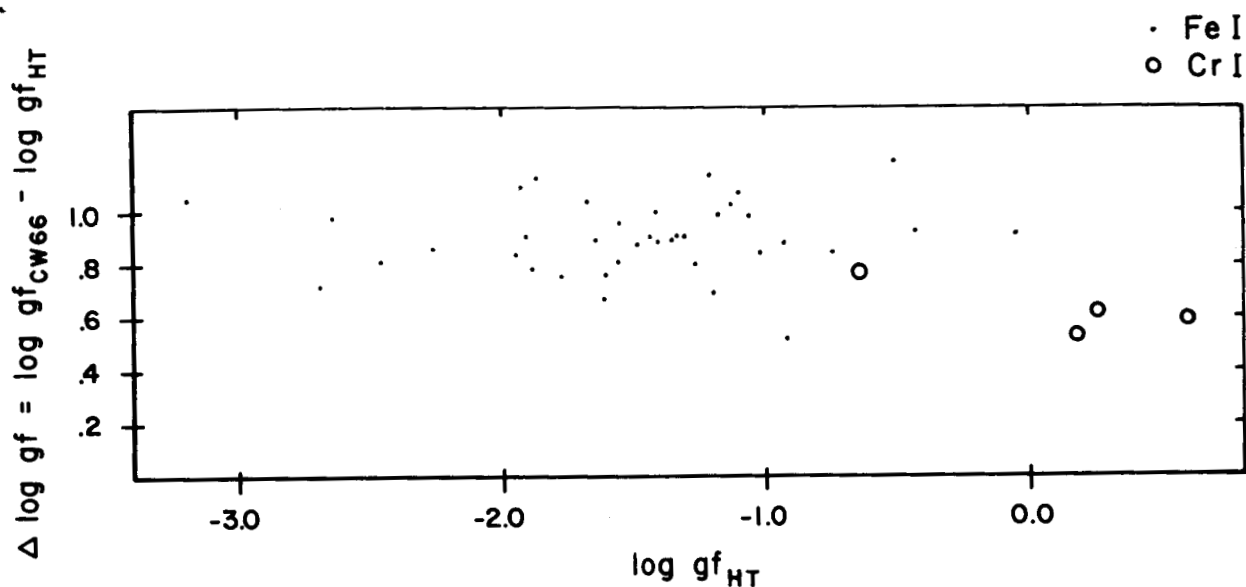


Figure 8a.- Plot of Figure 8 with corrected literature values.

There is no obvious trend in Fig. 9, where the difference $(\log gf_{lit} - \log gf_{meas})$ is plotted vs. wavelength. However, if a flat normalization function is used for the literature values (Fig. 9a) the standard deviation in Fig. 9 is reduced from .20 dex to .14 dex.[†]

The Cr gf-values measured are not numerous enough to justify an extensive discussion of their energy, line width and wavelength dependence. For reference, however, they are included in Figs. 6 through 9.

[†]Dex is defined as interval in powers of 10 (cf. Allen, 1964):
 .20 dex = $10^{.20}$.

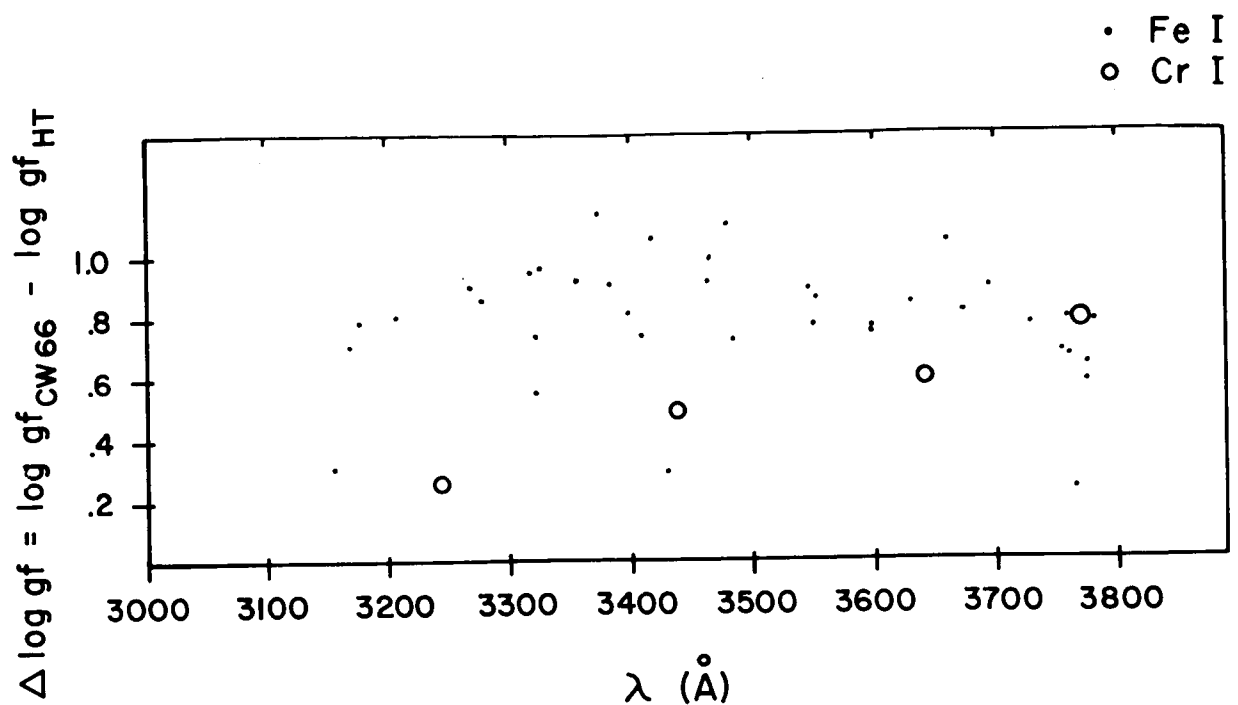


Figure 9.- A comparison of gf-values of Corliss and Warner (1966) with present measurements plotted vs. wavelength. The standard deviation is 0.20 dex.

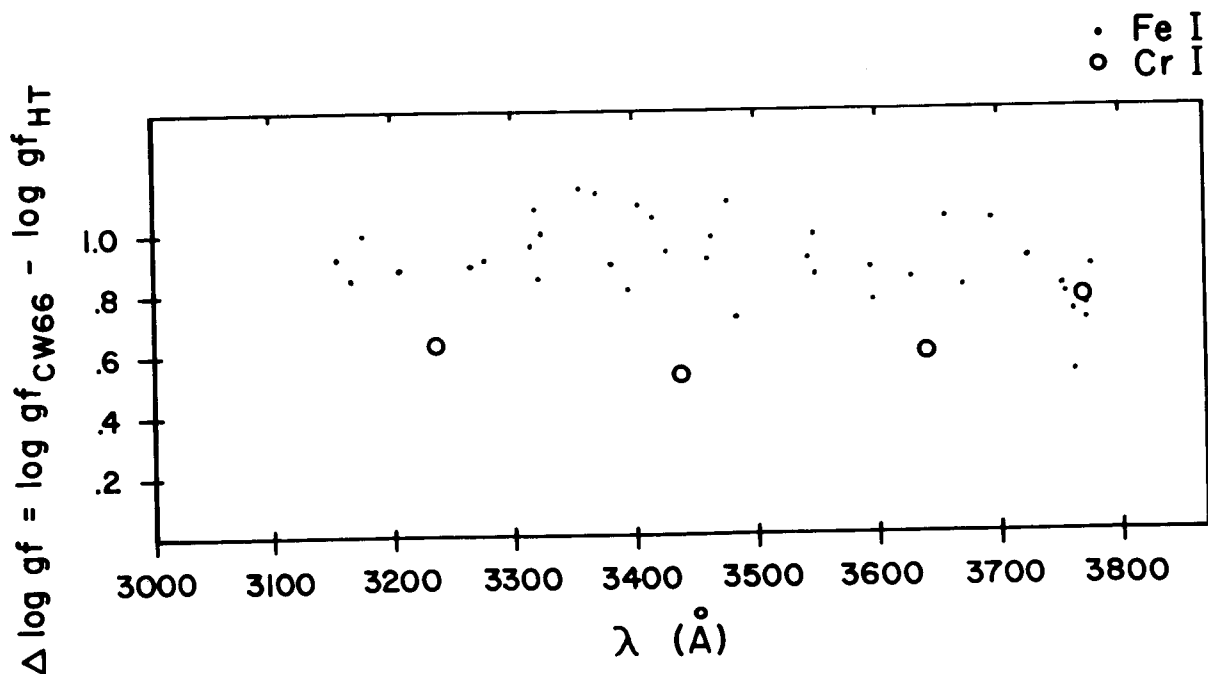


Figure 9a.- Plot of Figure 9 with corrected literature values. The standard deviation is 0.14 dex.

The literature values used for computing $\Delta \log gf$ as plotted in Figs. 6 through 9 are taken from Corliss and Warner (1966) for Fe I and from Corliss and Bozman (1962) for Cr I and Cr II. The further literature values listed in Table 1 were not numerous enough for a valid comparison of relative gf-values.

While the systematic deviation which shows up by comparing relative gf-values as a function of the upper excitation potential can easily be explained by the normalization function used for the literature gf-values, it is hard to find reasons why our absolute scales are approximately .90 dex and .64 dex lower than the ones used respectively by Corliss and Warner (1966) for Fe and by Corliss and Bozman (1962) for Cr.

In order to obtain the best estimate of the absolute scale for Fe, Corliss and Warner (1966) suggest that .10 dex be subtracted from their listed values. This would reduce the discrepancy to .80 dex. A more favorable comparison would result from basing the absolute scale on the data of Bell, Davis, King and Routly (1958) who revised older measurements of 12 Fe lines by R.B. King (1942) with new vapor pressure data. Here the discrepancy in absolute values would be .65 dex or a factor of 4.6; that is, virtually the same as with Cr.

The absolute scale for Fe I given by Prokofyev et al. (1964) is close to the one used by Corliss and Warner (1966). The absolute scales for Cr I and Cr II given by Allen and Asaad (1957) and by Shackleford (1965) respectively compare more favorably with our results. Both scales are lower than the National Bureau of Standards scales of Corliss et al., as pointed out by Allen and Corliss (1963) for Cr I (.40 dex) and by Shackleford (1965) for Cr II (.95 dex).

A careful analysis of the experiment has been made in order to find reasons for the discrepancy with the results of Corliss et al. (1962, 1966). The possibility that stray light in our spectrograph produced a noticeable error can be ruled out. Stray light does not affect absorption measurements strongly. It would need to be as intense as the continuum to reduce the equivalent width by a factor of two. An associated curve-of-growth telescoping effect is excluded by the large values of the parameter a which prevail in our experiment.

An error originating from the existence of a boundary layer is concluded to be negligible because no effect was seen on the temperature measurement. Since it was carried out on a resonance line, it was very sensitive to absorption by a boundary layer.

Also ruled out was the possibility that a lowering of the ionization potential appreciably depleted the neutral species. It was estimated that the ionization potential was lowered by only a few hundredths of an electron volt (Cooper, 1966). The resulting change in neutral number densities is well below 10 per cent for the conditions of this experiment.

The possibility of a loss of the Fe and Cr atoms during mixing, storing, and transferring of the gases was considered. No effect on f-values was seen when the storage time of the mixtures in the gas-handling system was varied from 4 to 42 hours.

In order to check the number density of atoms behind the reflected shock for losses in concentration, we evaluated hook spectra[†] which were obtained by one of us (M.H.) with the same gas-handling system and shock tube. With the known f-values of the three Cr I resonance lines at $\lambda\lambda$ 4254.3, 4274.8, 4289.7 Å (Lawrence, Link and King, 1965; improved atomic beam absorption technique) we could determine the number density of Cr in the shock-heated gas. The results of this test indicated that the actual number density in the shock-heated gas was within the

[†] A detailed description of the hook method experiments with the shock tube will be given in a forthcoming report.

experimental error (.08 dex) of the value expected. The average over several shocks even indicated a slight overabundance. Therefore we could not confirm a deficiency of a factor of 4.4 as suggested by the discrepancy of .64 dex in the gf-value absolute scale of Cr. Although this test is valid for Cr only, we assume that the identical procedure used for both Fe and Cr atoms did not introduce drastic differences in the number densities of iron and chromium.

On the other hand, it is known that an overpopulation of the ground state may exist even if the upper states are in local thermodynamic equilibrium. It is conceivable that the number density observed from resonance lines may be nearly correct while the number densities of the excited states are less than in the case of LTE. A criterion for the minimum electron density required for LTE between the ground state and the first excited state is given by Griem 1964 (Eqs. 6-60):

$$N_e \geq 9.10^{17} \left(\frac{E_{\text{res}}}{E_H} \right)^3 \left(\frac{kT}{E_H} \right)^{\frac{1}{2}} \text{ cm}^{-3}$$

E_{res} = energy of the lowest excited level

E_H = ionization potential of hydrogen (≈ 13.6 eV)

k = Boltzmann constant

N_e = electron density

Strictly speaking, this criterion is valid for ions only and, according to Griem, may be in error by up to a factor of three. A conservative estimate with $E_{\text{res}} = 3.1 \text{ eV}$ and $kT = 0.5 \text{ eV}$ (corresponding to a resonance line at 4000\AA and to a temperature $T = 5800^\circ \text{ K}$) yields $N_e \geq 1.6 \times 10^{15} \text{ cm}^{-3}$. This result is marginal since the corresponding electron densities obtained from the Saha equations were $3.3 \times 10^{15} \text{ cm}^{-3}$. However the condition may be relaxed by up to a factor of ten if the resonance lines are optically thick, as was the case here.

That LTE exists between the ground state and an excited state at 3.1 eV is indicated by a comparison of the line reversal temperature from the 3859.9\AA Fe resonance line with the temperature determined by hydrodynamic shock relations. The line reversal measurement in fact determines the Boltzmann temperature T_B of the relative population of the two combining levels according to

$$\log \frac{N_u}{N_l} = - \frac{5040}{T_B} \Delta E + \log \frac{g_u}{g_l}$$

ΔE = energy difference between states in eV

g_u, g_l = statistical weight of upper and lower state respectively

N_u, N_l = number density in upper and lower state respectively

With LTE this temperature differs from the hydrodynamic temperature by an amount corresponding to the enthalpy difference between a real and an ideal gas, or, in other words, corresponding to the excitation, ionization and dissociation energy of the real gas. In this experiment the observed differences between the two temperatures (average 4 per cent) can well be accounted for by the enthalpy difference. If the upper states were underpopulated (as compared to LTE) by a factor of 4.4 (.64 dex) the line reversal temperature would be about 20 per cent lower than the hydrodynamic temperature.

We therefore concluded that LTE was also established between ground state and the first excited levels, and that consequently the check on the number density by the hook method yielded valid results.

Finally, it should be mentioned that our absolute scale is supported by a recent solar abundance determination (Withbroe, 1967). It was found that our f -values for lines in the region 3000 to 4000 Å yield the same Fe abundance as Corliss and Warner's (1964) f -values for lines lying in the visible region. The uv f -values of these same authors yielded an overabundance of about $.6 \pm .2$ dex.

Although we were not able to find an explanation for the

difference between the absolute scales of Corliss and Warner (1964, 1966) and although the results of our experiment are supported by evidence from solar investigations, it is possible that an unknown source of error exists in the shock tube results. A definite conclusion however will only be justified when a reason for the discrepancy is found.

While the disagreement between the absolute scales should be investigated further, we suggest that the evidence presented on the normalization function for the population levels in an open arc established the need for a change of the National Bureau of Standards f-values (Corliss and Warner, 1964, 1966) for the Fe lines with upper excitation energies above $48\,000\text{ cm}^{-1}$.

ACKNOWLEDGEMENTS

We wish to thank Drs. W.H. Parkinson and E.M. Reeves for their continuous interest and support. Further thanks are due to Mr. D. Zitros for assisting with the electronics of the experiment and to Mssrs. K. Nicolas and G. Grasdalen for their help in reducing data.

The work reported was performed at Harvard College Observatory and was sponsored by the National Aeronautics and Space Administration through grant NsG-438. One of us (M.H.) is indebted to the European Space Research Organization (ESRO) and to the National Aeronautics and Space Administration for awarding him an ESRO/NASA International University Fellowship.

REFERENCES

Allen, C.W., 1964, Astrophysical Quantities (London: The Athlone Press).

Allen, C.W. and A.S. Asaad, 1957, M.N. 117, 36.

_____ and C.H. Corliss, 1963, M.N. 126, 37.

Charatis, G., 1961, Ph.D. Thesis, University of Michigan, Ann Arbor.

Cooper, J., Ed., 1966, Proceedings of Workshop Conference on the Lowering of the Ionization Potential and Related Problems of the Equilibrium Plasma, held at the University of Colorado, Nov. 12-13, 1965; JILA Report No. 79, (Boulder: University of Colorado).

Corliss, C.H. and W.R. Bozman, 1962, Nat'l. Bur. Stand. Monograph 53 (Washington, D.C. : Government Printing Office).

_____ and B. Warner, 1964, Ap. J. Suppl. 8, 395.

_____, 1966, J. Res. Nat'l. Bur. Stand. 70A, 325.

Davies, J.T. and J.M. Vaughan, 1963, Ap. J. 137, 1302.

Drawin, H.W. and P. Felenbok, 1965, Data for Plasmas in Local Thermodynamic Equilibrium, (Gauthier - Villars, Paris).

Garton, W.R.S., W.H. Parkinson, and E.M. Reeves, 1964, Ap. J. 140, 1269.

_____, 1965, Proc. Phys. Soc. (London) 88, 771.

Gaydon, A.G. and I.R. Hurle, 1963, The Shock Tube in High Temperature Chemical Physics (New York: Reinhold Publishing Corporation).

Hubenet, H., Ed., 1966, International Astronomical Union Symposium No. 26 on the Abundance Determination from Stellar Spectra, held at Utrecht, 1964, Academic Press, London and New York, p. 211.

Johnson, P.D., 1957, Rev. Sci. Instr. 28, 833.

Lawrence, G.M., J.K. Link and R.B. King, 1965, Ap. J. 141, 293.

Moore, C.E., M.G.J. Minnaert, and J. Houtgast, 1966, Nat'l. Bur. Stand. Monograph 61 (Washington, D.C. : Government Printing Office).

Onaka, R., 1958, Science of Light (Tokyo) 7, 23.

Pagel, B.E.J., 1965, Proc. 2nd Harvard-Smithsonian Conference
on Stellar Atmospheres (Cambridge, Massachusetts), 425.

Prokofyev, V.K., E.I. Nikonova, P.F. Gruzdev, and M.S. Frish,
1964, Crim. Ap. Obs. Izv. 31, 281.

Rich, J. and J. Flagg, 1966, Shock Tube Spectroscopy Laboratory
Scientific Report No. 12 (Harvard College Observatory).

Shackleford, W.L., 1965, J. Quant. Spectro. Radiat. Transfer.
5, 303.

Warner, B., 1964, M.N. of the Roy. Astron. Soc. 127, 413, and
ibid., 128, 63.

Wheaton, J.E.G., 1964, Appl. Optics 3, 1247.

Wiese, W.L., 1965, in Plasma Diagnostic Techniques, R.H. Huddle-
stone and S.L. Leonard, Eds. (New York and London: Academic
Press).

Wilkerson, 1961, Ph.D. Thesis, University of Michigan, Ann Arbor.

Withbroe, G.L., 1967, Shock Tube Spectroscopy Laboratory Scientific
Report No. 17 (Harvard College Observatory), in press.

Wurster, W. 1957, Rev. Sci. Instr. 28, 1030.

TABLE 1. LIST OF GF-VALUES

SPEC.	WL (A)	LEVELS (K)	MULT.	E1 (EV)	J-J	LOG (GF)	CW	PP	REMARKS
FE I	3156.275	26140-57814	578	3.24	3-3	-0.05	+0.25		
FE I	3168.858	19913-51461	160	2.47	2-3	-1.02	-0.32		
FE I	3176.366	21039-52512	258	2.61	2-1	-1.18	-0.40		
FE I	3207.089	19351-50523	159	2.40	5-6	-1.40	-0.60		
FE I	3268.234	17927-48516	95	2.22	1-1	-1.35	-0.45		
FE I	3278.741	19552-50043	144	2.42	1-1	-1.31	-0.46		
FE I	3278.741	20875-51365	250	2.59	3-3	-1.16			BLENDED
FE I	3317.121	18278-48516	139	2.28	2-1	-1.56	-0.60		BLENDED
FE I	3319.258	24119-54327	449	2.59	4-4	-1.10	-0.37		
FE I	3322.474	23711-53801	396	2.94	4-5	-0.75	-0.20		
FE I	3325.468	19788-49851	191	2.45	4-3	-1.41	-0.45		
FE I	3354.064	23052-52858	378	2.86	0-1	-1.21	-0.30		
FE I	3372.070	17550-47179	83	2.18	3-2	-1.87	-0.74		
FE I	3382.403	17550-47107	84	2.18	3-4	-1.55	-0.75		
FE I	3396.978	7728-37158	26	0.96	3-2	-2.46	-1.65		
FE I	3406.442	26406-55754	676	3.27	1-2	-0.51	+0.22		
FE I	3417.273	8155-37410	26	1.01	1-1	-3.19	-2.14		
FE I	3428.746	29056-58213	836	3.60	3-2	-0.43	-0.14		
FE I	3462.353	17727-46601	79	2.20	2-1	-1.91	-1.00		
FE I	3463.305	11976-40842	48	1.48	4-3	-2.64	-1.66		
FE I	3477.856	17927-46673	82	2.22	1-0	-1.92	-0.92	-0.85	
FE I	3483.006	7377-36079	24	0.91	4-3	-2.69	-1.97		
FE I	3544.631	21039-49243	239	2.61	2-2	-1.43	-0.55		
FE I	3548.037	24336-52512	496	3.02	2-1	-1.06	-0.29		
FE I	3549.868	12969-41131	48	1.61	2-1	-2.26	-1.40		
FE I	3595.308	23193-50999	322	2.87	2-2	-0.93	-0.17	-0.47	
FE I	3596.198	19621-47420	181	2.43	5-5	-1.61	-0.84		
FE I	3628.094	17727-45282	77	2.20	2-2	-1.95	-1.11		
FE I	3657.139	19552-46889	130	2.42	1-2	-1.68	-0.64		
FE I	3670.810	20038-47272	133	2.48	0-1	-1.56	-0.75		
FE I	3693.008	24339-51409	439	3.02	3-4	-1.13	-0.24		
FE I	3725.498	24575-51409	534	3.05	4-4	-1.33	-0.56		
FE I	3752.420	24507-51149	385	3.04	2-3	-1.27	-0.59	-0.62	BLENDED
FE I	3752.420	24507-51149	392	3.04	2-2	-1.27			BLENDED
FE I	3756.069	17550-44166	74	2.18	3-3	-1.89	-1.10		
FE I	3761.416	20875-47453	227	2.58	3-4	-1.6	-0.95		
FE I	3762.205	27167-53739	705	3.37	4-5	-0.92	-0.69		
FE I	3773.364	24575-51069	531	3.05	4-5	-1.78	-1.14		
FE I	3773.699	24507-50999	386	3.04	2-2	-1.20	-0.62	-0.68	
FE I	3777.061	24119-50587	432	2.99	4-3	-1.49	-0.71		
SPEC.	WL (A)	LEVELS (K)	MULT.	E1 (EV)	J-J	LOG (GF)	CB	AA	REMARKS
CR I	3237.729	23934-54811	114	2.97	4-4	+0.25	+0.50		
CR I	3238.087	24056-54930	114	2.98	5-5	-0.46			
CR I	3436.187	20524-49618	52	2.54	4-5	+0.17	+0.66	+0.25	BLENDED
CR I	3436.187	20524-49618	52	2.54	5-5	+0.17	+0.66	+0.25	BLENDED
CR I	3639.802	20520-47986	47	2.54	6-5	+0.59	+1.19	(-0.41)	
CR I	3768.734	20521-47047	43	2.54	3-2	-0.64	+0.14		
SPEC.	WL (A)	LEVELS (K)	MULT.	E1 (EV)	J'-J'	LOG (GF)	CB	SH	REMARKS
CR II	3382.683	19798-49352	3	2.45	2-2	-0.56	+0.39		
CR II	3421.20	19528-48750	3	2.42	0-0	-0.42	+0.51	-0.12	

TABLE 1., continued:

Remarks: $J' = J - 0.5$
If two lines are blended, gf-values are
computed for each line separately, assuming
no absorption from the other line.

Explanation of Symbols:

AA Allen and Asaad (1957) Arc
CB Corliss and Bozman (1962) Arc
CW Corliss and Warner (1966) Compilation
PR Prokofyev et al. (1964) Compilation
SH Shackleford (1965) Shock Tube